

Laser-induced refractive-index gratings in Eu-doped glasses

Frederic M. Durville, Edward G. Behrens, and Richard C. Powell

Department of Physics, Oklahoma State University, Stillwater, Oklahoma 74078-0444

(Received 25 April 1986)

Four-wave-mixing techniques were used to establish and probe refractive-index gratings in Eu^{3+} -doped silicate and phosphate glasses. When the Eu^{3+} ions are resonantly excited, superimposed transient and permanent gratings are formed. The former are characteristic of population gratings of excited Eu^{3+} ions while the latter are attributed to local structural modifications of the glass hosts. The time dependences of the grating buildup, decay, and erasure are reported as a function of temperature, laser power, and "write"-beam crossing angle for each of the samples. The results suggest the use of laser-induced gratings in these glasses in applications such as amplitude-modulated phase-conjugate reflectors.

I. INTRODUCTION

During the past ten years, a significant amount of work has been done in developing new optical devices designed to provide functions such as switching, modulation, phase conjugation, and bistability which are important in optical data processing applications. Glasses are very attractive materials for these devices because of the low cost and ease of fabrication compared to single crystals, and because they provide the opportunity for developing monolithic devices within systems based on fiber-optic transmission. Laser-induced refractive-index changes have been observed in several types of glasses¹⁻⁵ and used to produce holographic storage, narrow-band filters, optical switching, and phase conjugation. In most cases, the physical mechanism producing the photorefractive change has not been explained. We report here the observation of laser-induced, superimposed transient and permanent refractive-index changes in a rare-earth-doped glass. This provides a means for amplitude-modulated phase conjugation and switching. Details are presented of the results of four-wave-mixing (FWM) measurements in three different types of Eu^{3+} -doped glasses. For each sample it is found that resonant excitation of the Eu^{3+} ions with crossed

laser beams results in both transient population gratings and permanent holographic gratings. The dynamics of establishing and erasing these gratings were investigated as a function of laser power and temperature, and the results are interpreted in terms of a model based on vibrationally-induced structural modification of the host glass.

The glasses used in this work are europium pentaphosphate (EP), lithium phosphate (LP), and sodium silicate (NS). Their compositions are given in Table I and their spectroscopic properties have been reported previously.^{6,7} Similar measurements made on Eu^{3+} -doped borate, germanate, and fluoride glasses produced no strong, permanent FWM signal.

The experimental apparatus used for these experiments is shown in Fig. 1. The output of a Spectra Physics cw argon laser is split into two beams which are crossed inside the sample to form an interference pattern in the shape of a sine wave grating. The optical path lengths of both "write beams" are equal to within the coherence length of the laser. The wavelength is tuned to 465.8 nm in order to resonantly excite the 5D_2 level of the Eu^{3+} ions. The total power was varied between 10 and 160 mW by a variable neutral density filter. The interference pattern of the crossed laser beams creates a change in the re-

TABLE I. Summary of results.

Parameter	EP	Sample LP	NS
Network former (mol %)	83.3 P_2O_5	52.3 P_2O_5	72.0 SiO_2
Network modifier (mol %)		30.0 Li_2O 10.0 CaO 4.7 Al_2O_3	15.0 Na_2O 5.0 BaO 5.0 ZrO
Eu^{3+} content (mol %)	16.7 Eu_2O_3	3.0 Eu_2O_3	3.0 Eu_2O_3
τ_f (ms)	2.7	2.8	2.7
τ_r (ms)	2.67	2.85	2.86
t_{rise} (min)	15	30	0 ^a
ΔE_g (cm^{-1})	3983	2101	2890
ΔE_{e0} (cm^{-1})	4016	3213	614
$\Delta E'_f$ (cm^{-1})	2219	3824	699

^aAfter the "write" beams were turned off, a risetime of about 5 min was observed.

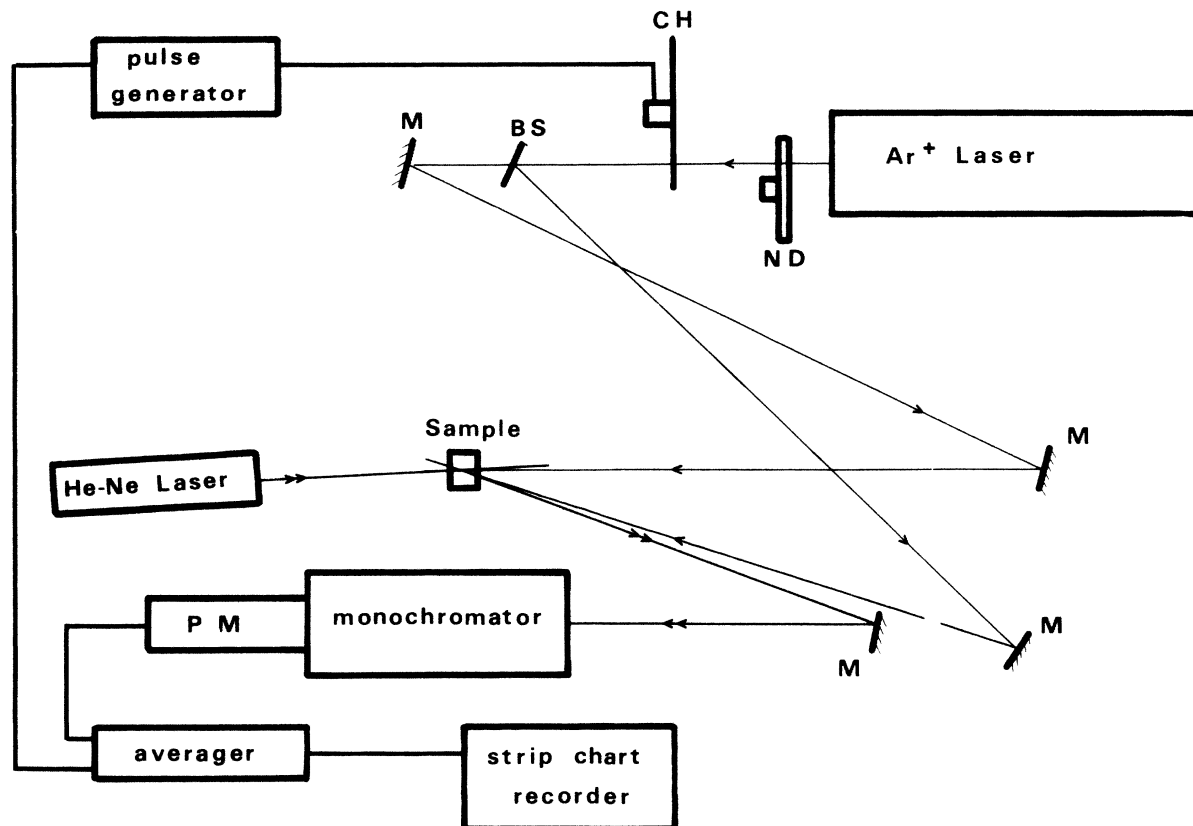


FIG. 1. Schematic diagram of the experimental setup used in the laser-induced grating experiments. ND—variable neutral density-density filter; CH—chopper; BS—beam splitter; M—mirror.

fractive index with the same shape. This acts like a “grating” and scatters the 10 mW “read” beam from a He-Ne laser at 632.8 nm. The maximum scattered signal beam is obtained at the Bragg condition for which the read beam is slightly misaligned from being counter propagating with one of the write beams and the signal beam is slightly off counter propagating with the other write beam. A mirror is used to pick off the signal beam and send it through a 0.25-m monochromator to eliminate sample fluorescence. The signal is detected by a Hamamatsu R1547 photomultiplier tube, processed by an EG&G/PAR signal averager, and read out on a strip chart recorder. For transient decay measurements, a chopper was used to cutoff the write beams while the decay of the signal beam was recorded. A pulse generator established the chopper frequency at about 20 Hz and triggered the signal averager. The erasure of the permanent grating was accomplished by exposure to a single laser beam at 465.8 nm and an EG&G/PAR lock-in amplifier was used to enhance the signal-to-noise ratio while measuring the signal beam scattered from the decaying permanent grating. For low-temperature measurements the sample is mounted in a cryogenic refrigerator with a temperature controller capable of temperature variation between about 10 and 300 K. For high-temperature measurements, the sample is mounted in a resistance heated furnace with a Chromel-Alumel thermocouple that can control the temperature between 300 and 775 K.

II. EXPERIMENTAL RESULTS

For all three samples, strong FWM signals were observed only if the write beams were tuned to resonance with an absorption transition of the Eu^{3+} ions. This shows that the mechanism producing the FWM signal is directly associated with the Eu^{3+} ions and that the impurity-induced nonlinear optical effect is significantly greater than the intrinsic nonlinear optical properties of the host glass.

Typical results for the time evolution of the FWM signals at room temperature are shown in Fig. 2. For both phosphate glasses the signal builds up slowly in time, reaching a maximum after about 15 min for EP and 30 min for LP, whereas for the silicate sample the signal immediately reaches maximum. The rate of signal buildup was found to be independent of write-beam laser intensity and grating spacing. For the same experimental conditions, the maximum signal strength was greatest for the EP sample and least for the NS sample. When the write beams were chopped off, the signal beams initially decayed exponentially with a decay time τ_t of the order of a few milliseconds as listed in Table I. For the EP and LP samples, the signal leveled off at about 70% of its maximum value and remained there indefinitely. For the NS sample the initial decay decreased to almost zero signal intensity, and this was followed by a buildup back to about 40% of the initial level as shown in Fig. 2(b). The

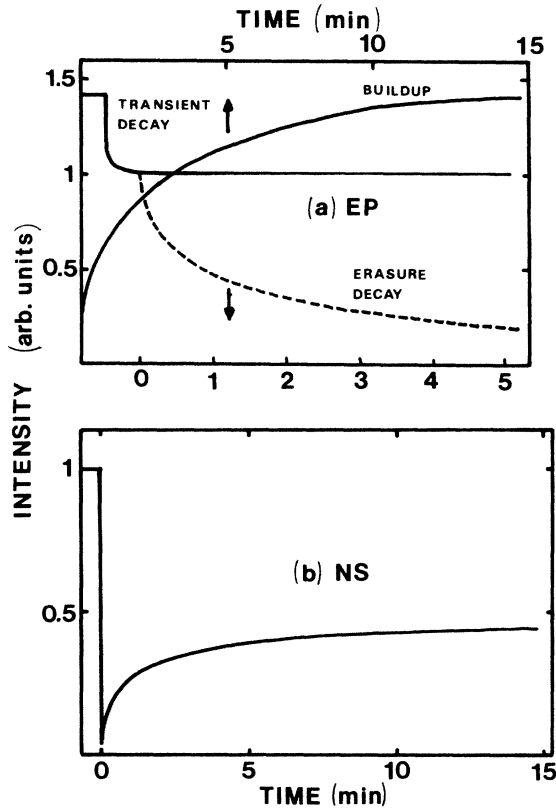


FIG. 2. Time evolution of the buildup, transient decay, and erasure of FWM signals in EP (a) and NS (b) glasses at 300 K. The total power of the laser write beams is 80 mW and the erase beam power is 40 mW.

permanent signal can be erased optically by switching on only one of the write beams in resonance with a Eu^{3+} transition. The rate of erasure varies with the intensity of the laser erase beam, with a typical erasure time shown in Fig. 2(a). The permanent signal can also be erased thermally by heating the samples up to about 390 K for

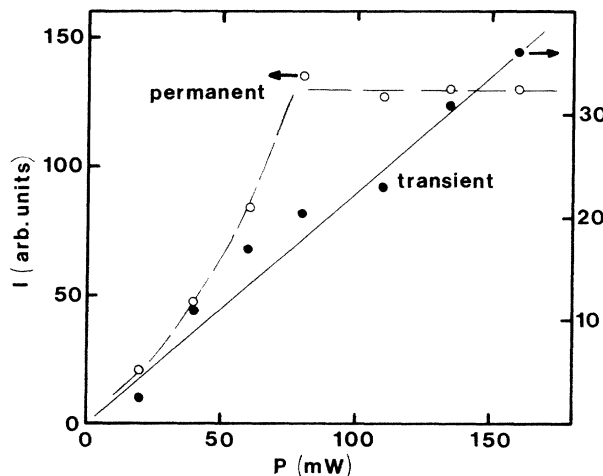


FIG. 3. Transient and permanent FWM signal intensities as a function of total write-beam laser power for EP at 300 K.

EP, 420 K for LP, and 520 K for NS. The total FWM signal can be treated as the superposition of read beams scattered from a transient grating and a permanent grating. Both components of the signal have intensities and decay rates which vary with laser power and crossing angle of the write beams, and with temperature, as described below.

Figure 3 shows an example of the variation of the permanent and transient signal intensities with the total laser power of the write beams. The intensity of the transient component of the signal increases linearly with laser power whereas the intensity of the permanent component of the signal initially increases approximately quadratically with laser power and then becomes independent of laser power above about 80 mW.

Figure 4 shows examples of the variations of the permanent and transient signal intensities with the crossing angle of the write beams. For all three samples, both signal components of the scattering efficiency decreases as the crossing angle increases. This is typical behavior for FWM signals and is associated with the length in which the probe beam interacts with the refractive-index grating

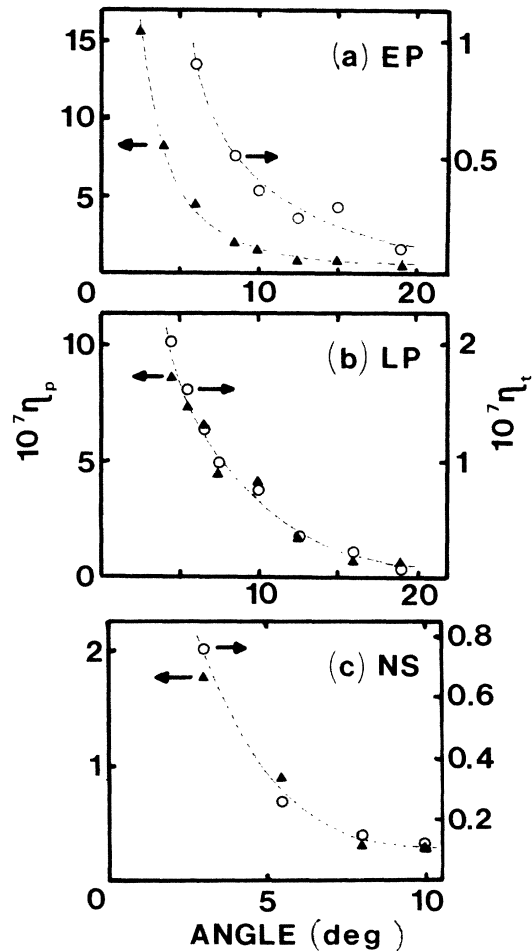


FIG. 4. Transient (\circ) and permanent (\blacktriangle) FWM signal efficiencies as a function of the crossing angle of the write beams in air at 300 K. (a) EP glass; (b) LP glass; (c) NS glass.

as well as the density of fringes and modulation depth of the grating. The exact form of the angular variation depends on the strength and mechanism of the beam coupling.

If a permanent grating is established at room temperature, the signal intensity of scattering from this grating decreases as temperature is increased. Typical results of this type of experiment are shown in Fig. 5. The maximum scattering intensities of both the permanent and transient gratings decrease as the sample temperature at which the grating is established increases. As shown in Fig. 6, the FWM signal components from both types of gratings decrease uniformly in the same way for the EP glass. This is initially true for the LP glass, but above about 350 K the transient signal can no longer be detected while the permanent signal intensity becomes independent of temperature. For the NS glass, both components of the FWM signal intensity initially increase with an increase in temperature, and then decrease uniformly in the same way for temperature increases above about 330 K. This behavior is associated with a change in the buildup of the permanent signal. Above about 330 K the signal in the NS glass has the same time evolution as the signal in the other samples at room temperature.

Both the transient signal decay rate and the permanent signal erasure rate were measured to be independent of the crossing angle of the laser write beams for all three samples. For the transient signal, the value of the grating decay rate is the same as the fluorescence decay rate of the

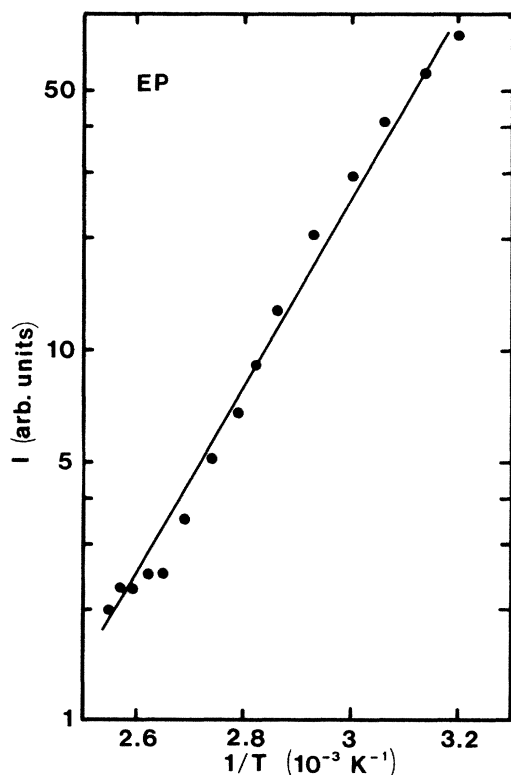


FIG. 5. Variation of the permanent FWM signal intensity as a function of temperature after laser-induced grating formation at 300 K in EP.

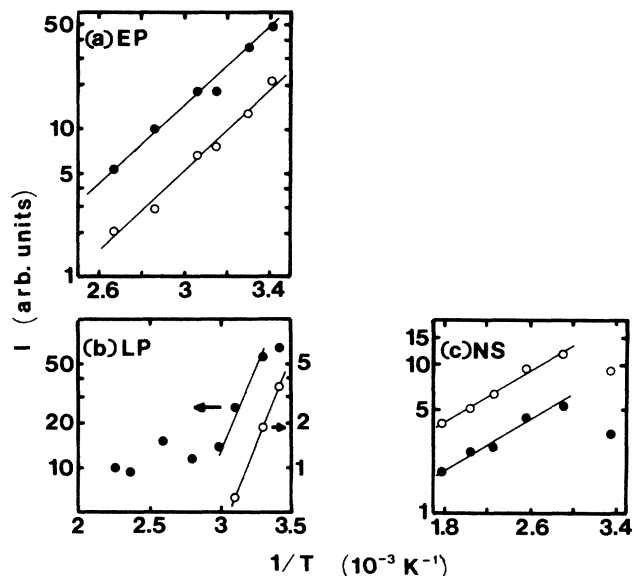


FIG. 6. Variation of the permanent (●) and transient (○) FWM signal intensities as a function of temperature of formation of the laser-induced gratings for (a) EP, (b) LP, and (c) NS samples. The total laser power of the write beams is 80 mW and the crossing angle in air is 7° .

5D_0 level of the Eu^{3+} ions, τ_f , as measured by independent experiments. These are listed in Table I.

The erasure rate for all three samples increases exponentially as the temperature at which the gratings are established and erased is increased. The rate of change of erase rate with temperature is significantly different for each of the samples as shown in Fig. 7.

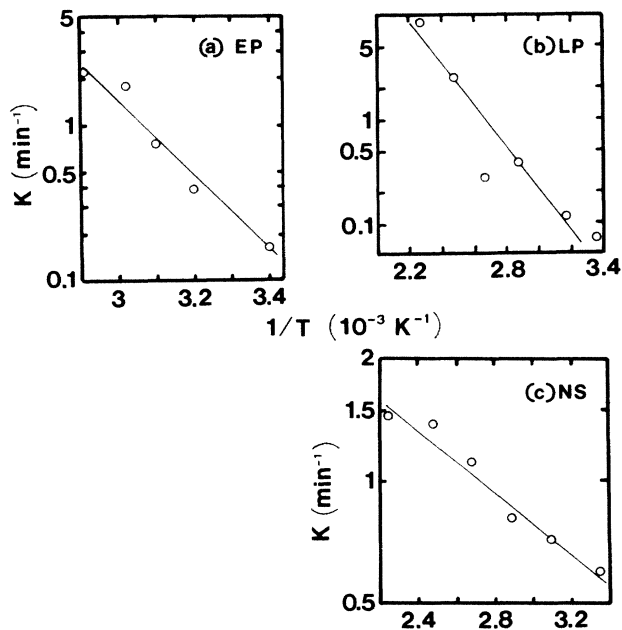


FIG. 7. Erasure decay rate of the permanent FWM signal as a function of temperature for (a) EP, (b) LP, and (c) NS at $\theta = 7^\circ$. The laser power in the erase beam is 40 mW.

III. INTERPRETATION OF RESULTS

The dynamics of the buildup and decay of FWM signals described in the previous section are consistent with scattering from two superimposed, laser-induced gratings. The FWM signal is proportional to the square of the change in the complex refractive-index induced in the material by the interference of the laser write beams,⁸ which in this case is the sum of the transient and permanent contributions to the change in the refractive index, $\Delta n \propto \Delta n_t + \Delta n_p$. If the transient component is assumed to decay exponentially with decay time τ_t , while the permanent component is time independent, the signal is described by

$$I_s \propto |\Delta n|^2 = |\Delta n_t|^2 \exp(-2t/\tau_t) + 2\Delta n_t \Delta n_p \exp(-t/\tau_t) + |\Delta n_p|^2. \quad (1)$$

The data shown in Fig. 2 imply that the first term in Eq. (1) is essentially negligible with respect to the last two terms.

A. Transient grating

Equation (1) predicts that the transient contribution to the FWM signal will decay exponentially with the decay time of the transient grating. This is consistent with the observed exponential transient decay. The fact that the FWM transient signal decay time is the same as the fluorescence decay time of the 5D_0 level of the Eu^{3+} ions, coupled with the fact that the FWM signal is observed only when a Eu^{3+} absorption transition is directly excited, shows that the transient grating is associated with a population grating of Eu^{3+} ions in the 5D_0 metastable state. Since the crossing angle of the laser write beams determines the grating spacing, the lack of any change of decay time with θ indicates that there is no long-range energy transfer in the excited state.

The linear increase in the transient component of the scattering efficiency with laser power should be described by the middle term in Eq. (1). The variation Δn_p due to the permanent grating is linear with laser power as discussed below. Thus, Δn_t associated with the transient grating appears to be independent of laser power at low powers and to vary linearly with laser power at high powers. It should be noted that the measurements of the signal intensities from the transient gratings took place after the signals from the permanent gratings had reached their maximum value. Thus the measured variation of transient grating scattering efficiency on laser power may be associated with the presence of the strong permanent grating.

The decrease in the intensity of the transient component of the scattering intensity with increasing write-beam crossing angle is the behavior typically observed for FWM signals.⁸ The scattering intensity of the transient signal decreases with increasing temperature in the same way as the intensity of the permanent signal. This implies that the refractive-index changes associated with the two gratings vary in the same way with temperature. The solid lines in Fig. 6 describe an exponential temperature variation

$$I = I_0 \exp(\Delta E_f'/kT), \quad (2)$$

where $\Delta E_f'$ is the activation energy and k is Boltzmann's constant. The values obtained for $\Delta E_f'$ for each sample are listed in Table I and their physical meaning is discussed below.

B. Permanent grating

Scattering of the read beam from the permanent grating contributes to the observed FWM signal through the third term in Eq. (1) as well as the second term describing the interference between the signals from the permanent and transient gratings. The fact that the grating takes times of the order of 15 min to build up and then shows no decay at room temperature over periods of days, indicates that the interference pattern of the laser write beams has produced some permanent change in the glass host. However, this change occurs only if the laser beams directly interact with a resonant transition of the Eu^{3+} ions.

The quadratic dependence of the signal intensity from the permanent grating on the power of the laser write beams as shown in Fig. 3, is consistent with the prediction of Eq. (1). The observed saturation shows that there is a limit to the glass modification that can take place. The decrease in scattering intensity with increasing write beam crossing angle shown in Fig. 4 is typical of FWM signals, as mentioned above.

The fact that the permanent grating can be erased, shows that the laser-induced change in the glass is reversible. The lack of change of the erasure decay rate with the crossing angle of the write beams indicates that the glass modification does not involve long-range migration of charge carriers. Since erasure can occur both thermally and by laser excitation of an absorption transition of the Eu^{3+} ions, the structural modification can be reversed with the Eu^{3+} ions in either the ground or excited state.

The observed temperature dependences of the signal intensities and erasure rates are consistent with exponential processes having activation energies ΔE_g for thermal erasure and ΔE_{e0} for thermally assisted optical erasure. The solid lines in Figs. 5–7 represent the best fits to the experimental data with an exponential expression. The values obtained for the activation energies are listed in Table I. The value of ΔE_g was obtained from the data in Fig. 5 and represents the activation energy of thermal erasure with the Eu^{3+} ions in the ground state. The value of ΔE_{e0} was obtained from the data in Fig. 7 and represents the activation energy of thermally assisted optical erasure with the Eu^{3+} ions in the excited state. The value of $\Delta E_f'$ was obtained from the data in Fig. 6 and represents the thermal activation energy associated with the grating formation process. This may be affected by concurrent erasure during grating formation, by thermal population of higher energy Eu^{3+} levels, or by thermally activated energy migration.

IV. DISCUSSION AND CONCLUSIONS

The FWM signal from the transient population grating observed here has significantly different properties from laser-induced population gratings studied previously.^{9–13}

For example, the decay rate of FWM signals associated with population gratings is usually reported to be twice the fluorescence decay rate, not equal to the fluorescence decay rate as observed here. The reason for these differences is clear from Eq. (1). We are not observing a FWM signal associated with an isolated population grating, but rather the signal associated with the interference between a permanent grating and a transient grating. According to Eq. (1), the intensity variations of the signal associated with this interference term will be affected by changes in the intensity of the permanent grating, while the decay will be described by the fluorescence decay rate. This accurately describes the observations for each of the three samples.

Permanent gratings can be created by crossed laser beams through several physical mechanisms. The most common mechanism is the photorefractive effect associated with the photoionization of defects and subsequent trapping of the free carriers.¹⁴ This type of mechanism can also lead to spectral hole burning, although this effect is seen only at low temperatures.¹⁵ The properties of the permanent gratings reported here are not consistent with this mechanism. The energy-level scheme for Eu^{3+} in these glass hosts is not compatible with an ionization transition at the laser wavelength used in these experiments. Multiphoton transitions are not probable with the low laser powers used and not consistent with the observed power dependence of the signal intensities. Also, no effects of refractive-index changes are observed with a single laser beam as they are for photorefractive materials. In addition, the fact that optical erasure occurs only when Eu^{3+} ions are resonantly excited is not consistent with the photoionization process. No spectral evidence was observed for the presence of Eu ions in valence states other than trivalent. Finally, the intensities of the two write beams were monitored as a function of time and no energy transfer between the two beams was observed. These two-beam mixing results show that the laser-induced grating is in phase with the laser interference pattern. This shows that the mechanism causing the grating is localized, which is not always true for gratings involving the migration of charge carriers.

Thermal processes can also produce refractive-index changes. Laser-induced stress-optic changes including some permanent effects have been seen in rare-earth-doped glasses.^{16,17} However, these observations were not dependent on having crossed laser beams and took place at higher powers than those used in our experiments. If local heating effects are the origin of the observed permanent grating, they should be described by the thermal conductivity equation,

$$-\partial Q/\partial t = \kappa A \nabla T, \quad (3)$$

where Q is the heat deposited by the laser in an area A , κ is the thermal conductivity of the glass, and ∇T is the local temperature gradient produced by this heat. For the glasses used in this work, the thermal conductivities are of the order of $10^{-2} \text{ cm}^{-1} \text{ K}^{-1}$. The laser power is less than 0.1 W with a beam cross-section area of less than 0.02 cm^2 . Using these conditions, the local rise in temperature predicted by Eq. (3) is only a few degrees. In addition,

these numbers overestimate ∇T because all of the laser power is not absorbed by the Eu^{3+} ions and converted to heat. Thus, standard local heating effects are not large enough to produce any permanent modifications of the glass.

The analysis given in the previous paragraph assumes a thermalized "phonon" bath in the host material. This condition is not satisfied in the local regions where the laser power is absorbed. The radiationless relaxation transitions of rare-earth ions in glasses have been shown to be "multiphonon" emission processes,¹⁸ each of which generates several high-energy "phonons," of the order of 1000 cm^{-1} . Since these are generated by the Eu^{3+} ions and the thermal diffusion in the glass host is slow, the phonons are localized thus creating a high level of nonthermalized vibrational energy around each ion. This can produce a local "effective temperature" which is extremely high compared to the thermal equilibrium temperature reached when these high energy phonons migrate away from their origin and become thermalized with the phonon modes of the host. For the radiationless relaxation processes of the Eu^{3+} ions under the excitation conditions of this experiment, local effective temperatures of the order of several thousand degrees Kelvin can be produced. This is easily enough to allow ionic motion over short ranges and thus produces a local structural modification of the host glass.

Based on the above discussion, we propose a model for the laser-induced permanent grating described by the configuration coordinate diagram shown in Fig. 8. It is assumed that the network forming and modifier ions of the glass host can arrange themselves in two possible configurations in the local environment of the Eu^{3+} ions, leading to double minima potential wells for the Eu^{3+} energy levels. For simplicity, only the three terms of the Eu^{3+} ions of direct relevance to the optical transitions of interest here, are shown in Fig. 8. The material is assumed to have a different index of refraction depending on which configuration is present. Under normal conditions of optical excitation and decay, the configuration coordinates appear as the solid lines in Fig. 8, and the ions will remain in the lower energy configuration, designated as I. The generation of local thermal energy may allow some of the ions to cross the potential barrier into configuration II, but it also will cause transitions in the reverse direction. The relative occupations of the two potential configurations will remain in thermal equilibrium, and as the local temperature returns to normal there will be a predominant occupancy of the lower energy potential well. However, with crossed laser beams, there is a gradient in the number density of high energy phonons resulting in a gradient in the local effective temperature. On a microscopic scale, the atomic motion involved in the configurational rearrangement can be described as an ionic conduction process involving only a few steps. In this picture the tendency of the vibrating atoms is to diffuse away from the peak of the temperature gradient. This gives a directional bias to the hopping of the atoms between sites of the different configurations. The resulting bias can be schematically represented by the change from the solid to the broken line potential curves in Fig. 8. This shifts lower potential minimum from configuration I to configuration II and

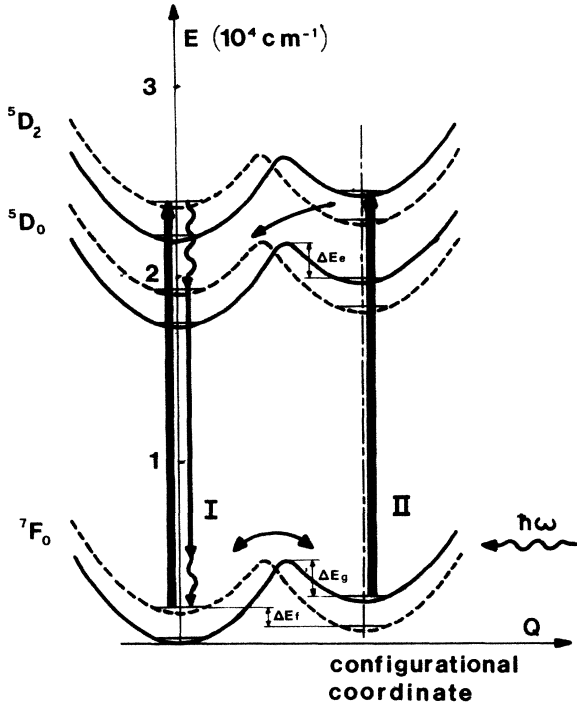


FIG. 8. Configuration coordinate model for laser-induced permanent gratings in Eu^{3+} -doped glass. The diagram shows only the relevant energy levels of the Eu^{3+} ions with two possible local configurations of the glass, I and II. The solid curves are for normal conditions of excitation and decay. The broken curves represent the change in potential coordinates due to the presence of crossed laser beams which creates a directional bias for ion motion. (See the text for explanation of transitions shown in the model).

thus builds up an increased population in configuration II. Even if this effect is quite small, over the several-minute time period of the grating buildup a significant change in configuration occupancy can be produced. When the crossed laser beams are turned off, the directional bias is removed and the configuration coordinates shift back to those shown by solid lines in Fig. 8, but the population built up in II remains. Since this "frozen in" distribution of excess occupation of II has the shape of the laser interference pattern, it appears to the probe beam as a refractive-index grating.

The transitions shown in Fig. 8 represent the processes involved in the formation and erasure of the permanent grating. Initially the ions predominantly occupy configuration I in the solid-line coordinate representation. During the grating formation period, crossed laser beams are tuned to resonance with the 7F_0 - 5D_2 transition of the Eu^{3+} ions. This produces the directional bias to shift the coordinate curves to the broken lines, as discussed above, and excites some of the Eu^{3+} ions to the 5D_2 level. The excitation energy is dissipated partially by radiative transitions to the ground terms and partially by radiationless transitions to the 5D_0 level through the emission of several high-energy phonons. The 5D_0 level also has radiative transitions to the ground terms. Most of the fluorescence transitions from both multiplets of the 5D term terminate

on the upper multiplets ($J=1-6$) of the 7F term and then decay through radiationless transitions to the 7F_0 ground-state multiplet. These processes generate several more high-energy phonons. The phonons produced through both excited-state and ground-state radiationless transitions provide the thermal energy needed to increase the occupancy of configuration II.

From this model, the refractive index can be written as the sum of the contributions from both configurations,

$$n = N_{\text{I}}n_{\text{I}} + N_{\text{II}}n_{\text{II}}, \quad (4)$$

where N_{I} and N_{II} are the populations of the two potential wells and n_{I} and n_{II} are the indices of refraction for the two configurations. For thermal equilibrium with the laser write beams on

$$N_{\text{I}}/N_{\text{II}} = \exp(\Delta E_f/kT), \quad (5)$$

where ΔE_f is the energy difference between the potential minima for the two configurations in the presence of the crossed laser beams and k is Boltzmann's constant. The FWM signal is proportional to the square of the difference of the index of refraction in the peak and valley region of the grating. If the valley regions of the grating are assumed to be all in configuration I, the FWM signal is given by

$$I \propto |\Delta n_{p-v}|^2 = N_p^2 |\Delta n_{\text{II-I}}|^2 \exp[2\Delta E_f/(kT)]. \quad (6)$$

The p and v subscripts refer to the peak and valley regions of the grating, respectively. This shows that the measured activation energy for the formation of the permanent grating $\Delta E_f'$ is twice the difference in the energy of the potential minima.

Erasure occurs thermally when the temperature is raised high enough to provide the energy ΔE_g needed to cross the ground-state potential barrier between configuration II and configuration I. With no crossed laser beams present, the solid coordinate curve is the relevant one in Fig. 8. This thermal energy allows the populations of the two potential configurations to redistribute themselves to the normal equilibrium case with predominant occupancy in configuration I. Optical erasure occurs with a single laser beam tuned to resonance with the 7F_0 - 5D_2 transition between the solid coordinate curves in configuration II. Relaxation back to the equilibrium population distribution can take place by several paths. Starting from the 5D_2 level in II, the excited Eu^{3+} ions relax back to the ground state and crossover to the I configuration which can take place at any of the levels occupied during the relaxation. Increasing the temperature will enhance optical erasure by making it easier to cross over the potential barriers such as the ΔE_e shown as an example in Fig. 8. Since crossover can occur with several different barriers, it is difficult to assign an exact meaning to the measured values of ΔE_{e0} . However, as for the thermal variation of the scattering, we can use a crude model to explain the thermal variation of the optical erasure rate. Assuming the excited ions relax to the 5D_0 state before any cross over to a different configuration occurs, the theory of Jortner and co-workers^{19,20} can be used. This was developed for radiationless transitions in large molecules

and has been successfully used to explain the nonradiative recombination of trapped excitons in chalcogenide glasses.²¹ At high temperatures and strong displacement of configuration minima, the approximate expression for the radiationless transition rate becomes

$$W_{II-I} = C^2 [4\pi kT / (hE_M)^2]^{1/2} \times \exp[-(E_M - \Delta E)^2 / (4E_M kT)], \quad (7)$$

where C is the matrix element for the transition and $(E_M - \Delta E)^2 / (4E_M kT)$ corresponds to the energy barrier between the two potential wells. This can be simplified in our case to

$$W_{II-I} = W_0 T^{1/2} \exp(-\Delta E_e / kT). \quad (8)$$

For our data the temperature-dependent prefactor is negligible and Eq. (8) is consistent with the observed results. However, the possibility of configuration crossover in the 5D_2 state, or between the 5D_2 state of II and the $^5D_{1,0}$ states of I, or in levels of the 7F_J manifold require that we interpret ΔE_{e0} as an "effective energy barrier" for crossover and not specifically associate it with a given level.

The difference in FWM properties between the EP and LP samples can be attributed to the significant difference in the Eu^{3+} concentration between the two samples. The difference between the LP and NS samples is more difficult to determine. Phosphate glasses have lower thermal conductivities, smaller nonlinear refractive indices, and different temperature coefficients of the refractive index compared to silicate glasses. To identify the properties most important in producing the observed FWM characteristics, different combinations of glass hosts and rare-earth ions need to be investigated.

Two-level systems have been proposed previously to explain other physical properties associated with vibrational

modes in glasses.²² However, the effects of having two possible configuration potentials have generally been considered only at very low temperatures. Laser-induced refractive-index changes in glasses have been observed for different types of glasses under different experimental conditions and the results attributed to bond rearrangements associated with trapped exciton effects.³⁻⁵ This mechanism is not consistent with the results observed in our experiments. The model proposed here appears to be consistent with all of the observed characteristics of the laser-induced permanent grating. However, to verify this model more experimental data obtained on different kinds of glasses is needed.

The results reported here represent the first observation of an interference effect in an FWM signal due to the superposition of a transient population grating and a permanent grating due to structural modification of the host. Producing FWM signals in glasses of this type may be useful in optical systems involving fiber-optic transmission since it should be possible to use the techniques described here to establish phase conjugate mirrors and optical switches directly in the glass fibers. Finally, understanding the details of the mechanism for forming the laser-induced permanent gratings may lead to a better understanding of the local structural and vibrational properties of these types of glasses.

ACKNOWLEDGMENT

This research was supported by the U.S. Army Research Office and by the National Science Foundation under Grant no. DMR-82-16551. The authors gratefully acknowledge the help of M. J. Weber in providing the samples used in this work and the benefit of discussions concerning these results with G. S. Dixon.

- ¹J. Bures, J. Lapierre, and D. Pascale, *Appl. Phys. Lett.* **37**, 860 (1980).
- ²K. O. Hill, Y. Fujii, D. C. Johnson, and B. S. Kawasaki, *Appl. Phys. Lett.* **32**, 647 (1978); B. S. Kawasaki, K. O. Hill, D. C. Johnson, and Y. Fujii, *Opt. Lett.* **3**, 66 (1978).
- ³R. A. Street, *Solid State Commun.* **24**, 363 (1977).
- ⁴K. Tanaka and A. Osajima, *Appl. Phys. Lett.* **38**, 481 (1981).
- ⁵J. H. Kwon, C. H. Kwak, and S. S. Lee, *Opt. Lett.* **10**, 568 (1985).
- ⁶G. S. Dixon, R. C. Powell, and X. Gang, *Phys. Rev. B* **33**, 2713 (1986).
- ⁷X. Gang and R. C. Powell, *J. Appl. Phys.* **57**, 1299 (1985).
- ⁸J. Feinberg, in *Optical Phase Conjugation*, edited by R. A. Fisher (Academic, New York, 1983), p. 417.
- ⁹H. J. Eichler, J. Eichler, J. Knof, and Ch. Noack, *Phys. Status Solidi A* **52**, 481 (1979).
- ¹⁰P. F. Liao, L. M. Humphrey, D. M. Bloom, and S. Geschwind, *Phys. Rev. B* **20**, 4145 (1979); P. F. Liao and D. M. Bloom, *Opt. Lett.* **3**, 4 (1978).
- ¹¹J. R. Salcedo, A. E. Siegman, D. D. Dlott, and M. D. Fayer, *Phys. Rev. Lett.* **41**, 131 (1978).
- ¹²J. K. Tyminski, R. C. Powell, and W. K. Zwicker, *Phys. Rev.*

B **29**, 6074 (1984).

- ¹³A. M. Ghazzawi, J. K. Tyminski, R. C. Powell, and J. C. Walling, *Phys. Rev. B* **30**, 7182 (1984).
- ¹⁴P. Gunter, *Phys. Rep.* **93**, 199 (1982).
- ¹⁵A. Winnacker, R. M. Shelby, and R. M. Macfarlane, *Opt. Lett.* **10**, 350 (1985); R. M. Macfarlane and R. M. Shelby, in *Coherence and Energy Transfer in Glasses*, edited by P. A. Fleury and B. Golding (Plenum, New York, 1984), p. 189.
- ¹⁶L. G. DeShazer (private communication).
- ¹⁷C. L. Sauer, Ph.D. thesis, University of Southern California, 1980.
- ¹⁸C. B. Layne, W. H. Lowdermilk, and M. J. Weber, *Phys. Rev. B* **16**, 10 (1977).
- ¹⁹K. F. Freed and J. Jortner, *J. Chem. Phys.* **52**, 6272 (1970).
- ²⁰R. Englman and J. Jortner, *Mol. Phys.* **18**, 145 (1970); R. Englman, *Nonradiative Decay of Ions and Molecules in Solids* (North-Holland, Amsterdam, 1979).
- ²¹N. F. Mott, E. A. Davis, and R. A. Street, *Philos. Mag.* **32**, 961 (1975).
- ²²P. W. Anderson, B. I. Halperin, and C. M. Varma, *Philos. Mag.* **25**, 1 (1972).